Marine Geology 401 (2018) 2–16

Contents lists available at ScienceDirect

Marine Geology

journal homepage: www.elsevier.com/locate/margo

Sediment accumulation and retention of the Changjiang (Yangtze River) subaqueous delta and its distal muds over the last century

Jianjun Jia[a,b,*], Jianhua Gao[c], Tinglu Cai[b], Yan Li[d], Yang Yang[a], Ya Ping Wang[a], Xiaoming Xia[b], Jun Li[e], Aijun Wang[f], Shu Gao[a,**]

[a] State Key Laboratory for Estuarine and Coastal Research, East China Normal University, Shanghai 200062, China
[b] State Research Centre for Island Exploitation and Management, Second Institute of Oceanography, State Oceanic Administration, Hangzhou 310012, China
[c] Ministry of Education Key Laboratory for Coast and Island Development, Nanjing University, Nanjing 210093, China
[d] State Key Laboratory of Marine and Environmental Science, Xiamen University, Xiamen 361005, China
[e] Qingdao Institute of Marine Geology, Qingdao 266071, China
[f] Open Laboratory for Coast and Ocean Environmental Geology, Third Institute of Oceanography, State Oceanic Administration, Xiamen 361005, China

ARTICLE INFO

Editor: E. Anthony

Keywords:
Sediment retention index
Material budgeting
Deposition rate
Subaqueous delta
Shelf mud deposits
The Changjiang River

ABSTRACT

Mega-deltas are major sinks of river-borne sediments and important sources of terrigenous sediments for open shelves. Their evolution has far-reaching impacts on adjacent coastal waters, from the point of view of along-shelf morphodynamics and biogeochemistry. However, the complex budgeting patterns of input, storage, bypass, and final accumulation of sediment are still poorly understood. The Changjiang (Yangtze River) in China is among the world's largest river systems, not only in terms of water and sediment discharges but also the massive amount of sediment deposited in its subaqueous delta and distal muds. Here we discuss about the along-shelf sediment redistribution in the Changjiang Subaqueous Delta and Distal Muds (CSDDM) over the last century. For the purpose of understanding its spatial diversity in detail, we divided the study area into three spatially connected parts, namely the Changjiang subaqueous deltaic mud (CJM), the Zhejiang inner-shelf mud (ZJM), and the Fujian inner-shelf mud (FJM). The concept of sediment retention index helps understand the overall evolution of this mega-delta. Hydrological survey data from the peripheral rivers and short marine-sediment cores are used to evaluate the amount of sediment supplied to and deposited in the study area. The results show that over the last century, the rate of sediment supply to the CSDDM reached ~645 Mt $year^{-1}$ on average (ranging between 535 and 725 Mt $year^{-1}$), while the total sediment deposition in the CSDDM reached ~683 Mt $year^{-1}$ on average (390–976 Mt $year^{-1}$), with the ratio for the deposits in the CJM, ZJM and FJM being close to 3:5:2. As such, the input and output of sediment were generally in balance. The sediment retention indices are estimated to be 0.35, 0.86 and 1.00 for CJM, ZJM and FJM, respectively. This study contributes to our knowledge of marine sediment fluxes, facilitates a better understanding of the growth and development of mega-deltas under system regime shifts, and helps identify a sustainable development model for areas of high population density, heavy economic activity and rapid urbanization.

1. Introduction

Large-river deltas are contributors to clastic sediment masses on continental shelves (Driscoll and Nittrouer, 2000; Milliman and Farnsworth, 2011), with their delta-front estuaries representing a critical interface for material fluxes that have a far-reaching influence on marine biogeochemistry and ecosystems (Bianchi and Allison, 2009), and the evolution of such deltas can affect nearby coastal zones (Gao and Collins, 2014). Further, Mega-deltas have been a focus for human civilization in the Holocene period. It is the transport and deposition of massive, catchment-derived sediment in deltas that create new land that support human habitation and economic development.

The Changjiang (Yangtze River) is among the largest rivers in the world in terms of its drainage basin area (180×10^4 km^2), length (6300 km), runoff (9000×10^8 m^3 $year^{-1}$), and sediment discharge (500 Mt $year^{-1}$; Milliman and Farnsworth, 2011). Behind these physical parameters, the Changjiang Subaerial Delta is inhabited by 150 million people, and the gross domestic product of the region was US$2 trillion in 2014 (NDRC, 2016). Furthermore, the spatial scale of the Changjiang subaqueous delta and the related distal muds (CSDDM) is

* Correspondence to: J. Jia, State Key Laboratory for Estuarine and Coastal Research, East China Normal University, Shanghai 200062, China.
** Corresponding author.
E-mail addresses: jjjia@sklec.ecnu.edu.cn (J. Jia), sgao@sklec.ecnu.edu.cn (S. Gao).

https://doi.org/10.1016/j.margeo.2018.04.005
Received 30 July 2017; Received in revised form 4 April 2018; Accepted 10 April 2018
Available online 12 April 2018
0025-3227/

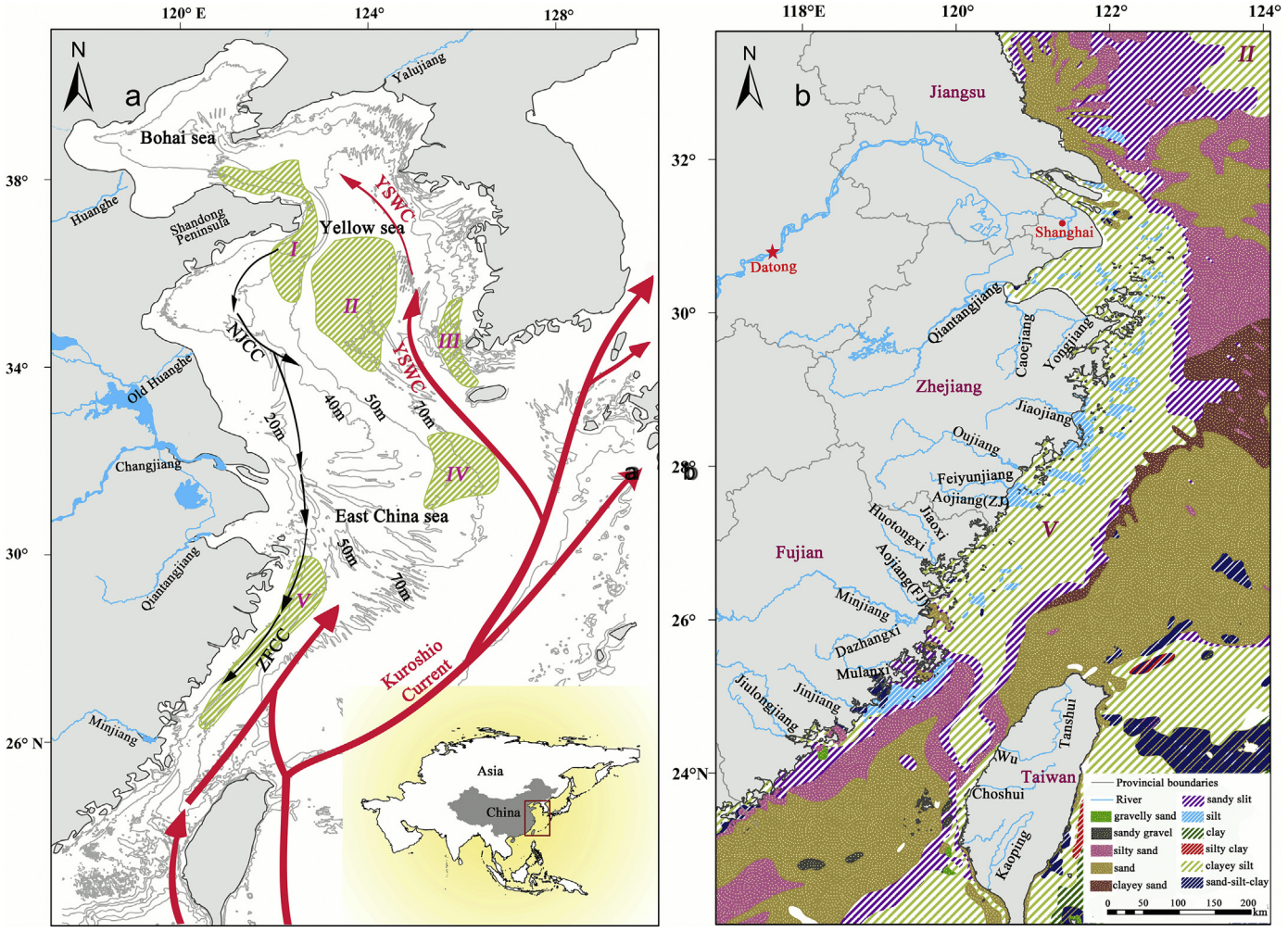

Fig. 1. (a) Location map showing the regional circulation pattern (adapted from J.P. Liu et al., 2007) and locations of mud deposition (adapted from Gao et al., 2016). (b) Surficial sediment types in the study area (after Shi, 2012) and the major rivers running into the sea.
NJCC = Northern Jiangsu Coastal Current, ZFCC = Zhejiang Fujian Coastal Current, TWC = Taiwan Warm Current, YSWC = Yellow Sea Warm Current.
I: Huanghe distal mud; II: isolated mud patch in the central Yellow Sea; III: Huskan Mud Belt in the SE Yellow Sea; IV: isolated mud patch in the south of Cheju Island; V: Changjiang distal mud.

large, implying a massive amount of sediment transferred by the delta. The CSDDM forms a 1000 km-long mud belt system, extending from the Changjiang estuary in the north towards the middle Taiwan Strait in the south, covering an area of around 0.1×10^6 km^2 (Qin, 1963, 1996; J.P. Liu et al., 2007; Liu et al., 2018; see Fig. 1). The eastern boundary of the distal muds roughly follows the 50–70 m bathymetry. The sediments are derived mainly from the Changjiang, the smaller rivers of Zhejiang and Fujian provinces, and the west coastal rivers of Taiwan (DeMaster et al., 1985; Qin et al., 1996; J.P. Liu et al., 2007; Liu et al., 2008; Xu et al., 2009). The total mass of mobile mud over the region is around 800 Mt (Wang et al., 2016).

Two important phases of change have been observed within the Changjiang system during the last 100 years (Wang et al., 2008; Gao et al., 2015a). The first phase occurred after the Second World War, when agricultural/industrial development and urbanization began to gradually change the supply and flux of sediment from the Changjiang catchment. The second phase, starting from the 1980s, was characterized by ambitious and far-reaching anthropogenic activities, such as the Three Gorges Dam Project in the main stream and the Deepwater Channel Regulation Project in the Changjiang Estuary. During the past century, the amount of sediment transported from the Changjiang to the sea reached its peak on a millennium scale, and possibly even for the Holocene (Lin and Pan, 2005; Wang et al., 2008; Gao et al., 2015a), then followed by a sharp decline (MWR 2000–2016; Yang et al., 2011; Fig. 2). The continuous growth of the Changjiang Delta was then threatened (Li et al., 2007; Gao, 2010; Yang et al., 2011).

Although the Changjiang catchment is well studied in terms of its sediment yield, our knowledge of the CSDDM sediment dynamics remains limited (Qin, 1963; Milliman and Yang, 2014). Century-scale dating techniques using natural and artificial radioactive isotopes (e.g., ^{210}Pb and ^{137}Cs) are a vital tool in evaluating the sedimentology of estuaries and near-shore environments (Goldberg, 1963; Nittrouer et al., 1979; Appleby and Oldfield, 1983). The objective of this study is to assess the supply of sediment and analyze the sediment retention patterns of the CSDDM over the last century, based on ^{210}Pb dating of tens of short cores obtained in this study, together with the collection of > 200 short cores with ^{210}Pb and ^{137}Cs dating and collected hydrological data of riverine sediment discharge. The results of this work will advance our knowledge of morphodynamic behaviors of mega-deltas under system regime shifts. More importantly, with the drastic decrease in sediment supply and the unprecedented human impacts on the river-delta-shelf system, questions about the sustainable development of mega-deltas must be addressed (Gao, 2007; Nicholls and Cazenave, 2010). The solutions to such questions will have global implications, especially for areas with high population density, heavy economic activity and rapid urbanization, e.g., the Zhujiang (Pearl River) Delta in

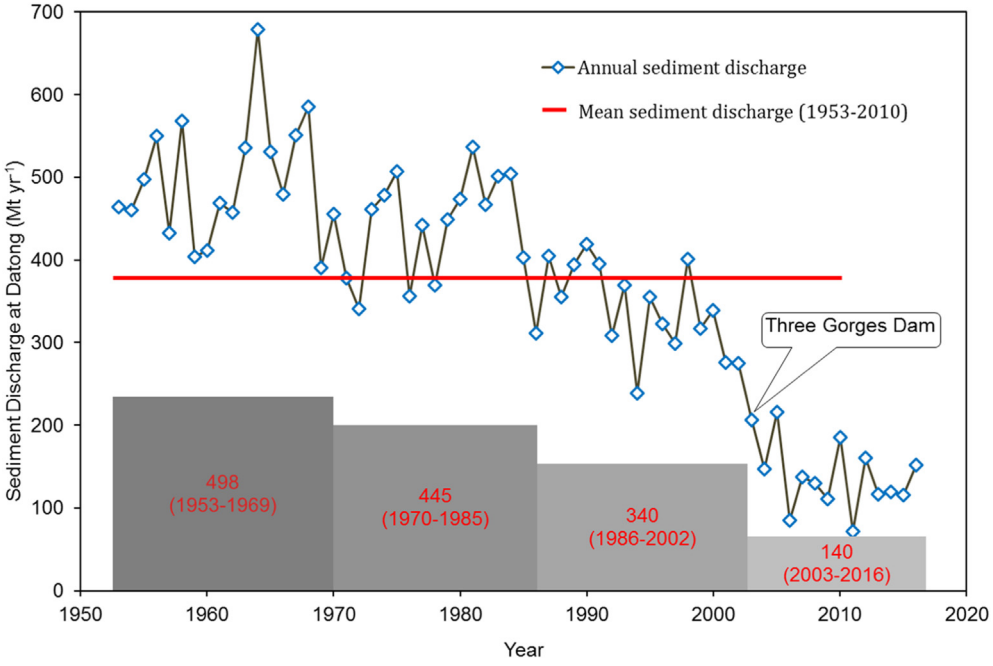

Fig. 2. Annual (blue diamonds) and mean (red line, 390 Mt year^{-1}) sediment discharge measured at Datong station on the Changjiang from 1953 to 2016 (data source: MWR 2000–2016). Four stages of stepwise reduction are distinguished (according to Gao et al., 2015b) and are indicated by the gray bars with red labels showing the corresponding mean fluxes of sediment and the time span. (For interpretation of the references to colour in this figure legend, the reader is referred to the web version of this article.)

China and the Mekong River Delta in Vietnam.

2. Materials and methods

2.1. Sampling

An 80-ton fishing vessel, *Suruyu 3259*, was used for cruises in December 2013, March 2014, and September 2015. Sediment samples were collected within the Changjiang Estuary and along the Zhejiang and Fujian coastal waters. Clam-type mud samplers were used to collect surficial samples, and gravity piston samplers were used to collect short core samples (1.5–2.0 m long). A total of 51 core samples were collected (Fig. 3). A Trimble Geo-XT portable DGPS was used for positioning during the field work, with a positioning accuracy of ~10 m.

2.2. Laboratory treatment

The experimental analysis was conducted at the MOE Key Laboratory of Coastal and Island Development, Nanjing University, China. Each short core was split vertically into two portions, and both were carefully cut at 2-cm intervals. Subsamples of one portion were used for grain-size analysis using a Malvern Mastersizer 2000 laser particle analyzer, and those of the other portion were prepared for ^{210}Pb analyses.

The ^{210}Pb activity was measured via the α-active granddaughter, ^{210}Po (Tanner et al., 2000). The samples were dried in a vacuum-freeze dryer and sifted through a 4 ϕ (63 μm) mesh sieve. The fine particles were then ground, dried, weighed, and sealed in plastic containers for one year or more. The purpose of the pre-treatment is to reduce the impact of particle size on the ^{210}Pb activity measurement and to achieve secular equilibrium between ^{210}Pb and ^{210}Po.

Chemical treatment of the samples before detecting ^{210}Pb activities followed the procedure described by Wang et al. (2014). In brief, the ^{210}Pb activity was measured with an OCTETE 576A alpha spectrometer after aqua regia extraction and electrode positioning. This step was followed by calculating the amount of excess ^{210}Pb (^{210}Pb$_{ex}$) by subtracting the background ^{210}Pb activity from the ^{210}Pb activity measured in each layer (for details of the procedures followed in these laboratory experiments, see Wang et al. (2014).

2.3. ^{210}Pb dating and sedimentation rate determination

The use of the natural radioactive isotope ^{210}Pb for dating and determining century-scale sedimentation rates has been discussed in numerous studies (Goldberg, 1963; Koide et al., 1972; Nittrouer et al., 1979; Appleby and Oldfield, 1983). Briefly, ^{210}Pb is the eventual decay product of ^{222}Rn (an inert gaseous element with a half-life of 3.83 d), which is the daughter isotope of ^{226}Ra (half-life of 1622 years). ^{210}Pb has a half-life of 22.3 years, and the ^{210}Pb in natural sediment is derived mainly from two sources: unsupported and supported. The unsupported ^{210}Pb is mainly from atmospheric deposition as the decay daughter of ^{222}Rn, then absorbed by suspended particulates and eventually deposited in sediment. The supported ^{210}Pb is the decay daughter of ^{226}Ra in sediments. Without subsequent disturbances or erosion, the unsupported ^{210}Pb behaves in accordance with the principle of radioactive decay. According to this principle, the ages of horizons within the sediment were inferred based on the measurements of the unsupported ^{210}Pb radioactivity. By combining the depths of the dated horizons and the density of the sediment, the mass accumulation rates (g cm^{-2} year^{-1}) or sedimentation rates (cm year^{-1}) were calculated.

Two widely employed models for calculating ^{210}Pb dates have been proposed, i.e., the constant rate of supply (CRS) model and the constant initial concentration (CIC) model. Generally, the CRS model is more effective for the environments where the sediment source changes over time (Appleby and Oldfield, 1983). Therefore, the CRS model is used to calculate the sedimentation rate in this study. The CRS model assumes that the atmosphere supplies the sediment suspended in the water column with ^{210}Pb at a constant rate, regardless of any variations in the sediment accumulation rate. The CRS-determined ^{210}Pb age is deduced by:

$$\sum A_i = \left(\sum A_b\right)\left(1 - e^{-\lambda \frac{M}{R}}\right) \quad (1)$$

$$\frac{M}{R} = -\frac{1}{\lambda}\ln\left(1 - \frac{\sum A_i}{\sum A_b}\right) \quad (2)$$

where ΣA_b is the unsupported ^{210}Pb inventory of the entire core, ΣA_i is the unsupported ^{210}Pb inventory below the subsample being dated, λ is the decay constant for ^{210}Pb (0.03114 year^{-1}), M is the mass depth (g cm^{-2}), and R is the mass accumulation rate (g cm^{-2} year^{-1}). Eq. (2)

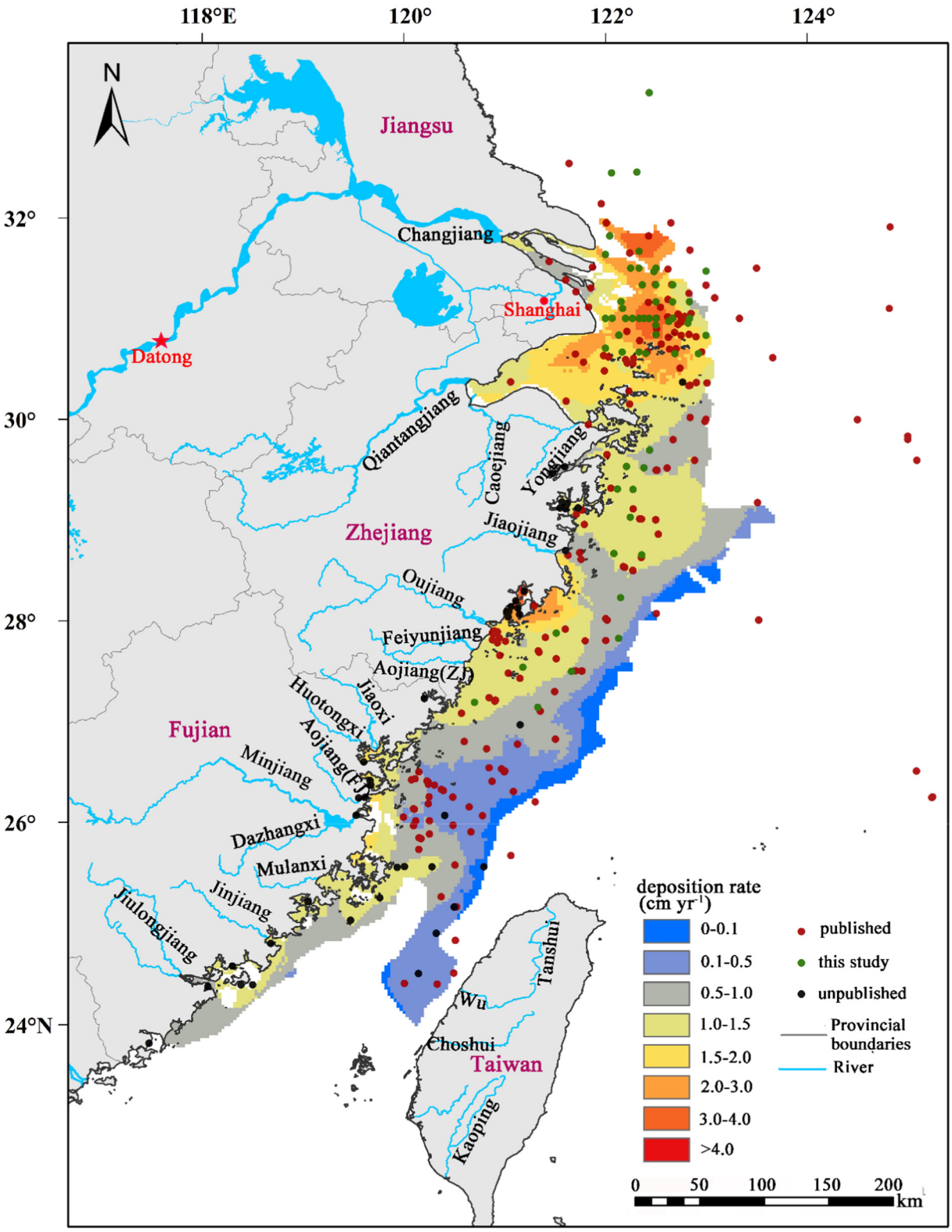

Fig. 3. Distribution of modern sedimentation rates within the study area and the planar distribution of sedimentation rates after interpolation. (Data sources: published data are from Chen et al. (1982, 2004); Alexander et al. (1991); Xie et al. (1994); Huh and Chen (1999); Su and Huh (2002); Oguri et al. (2003); Xia et al. (1999, 2004); Duan et al. (2005); Zhang et al. (2005, 2009, 2016); Yang and Chen (2007); Wang et al. (2008); Zhang (2008); Dong et al. (2009); Feng et al. (2009); Jin et al. (2009); Huh et al. (2011); Youn and Kim (2011); Wang et al. (2012, 2013); Cheng et al. (2013); unpublished data are from M. Liu (2009); Y. Liu (2009); Chen (2010); Xia (2011); Xie (2013)).

can be rewritten as a function of depth and the sedimentation rate (cm year^{-1}) when the dry bulk density is assumed to be constant throughout the core:

$$\frac{H}{S} = -\frac{1}{\lambda}\ln\left(1 - \frac{\sum A_i}{\sum A_b}\right) \tag{3}$$

where H is the depth (cm) and S is the sedimentation rate (cm year^{-1}). If the normalized excess ^{210}Pb activity is used instead of the excess ^{210}Pb activity, then we have

$$\ln\left(1 - \frac{\sum \frac{A_i}{A_0}}{\sum \frac{A_b}{A_0}}\right) = -\frac{\lambda}{S}H \tag{4}$$

where A_0 is the initial excess ^{210}Pb activity. Therefore, the sedimentation rate is estimated using the slope of the linear regression between $\ln\left(1 - \frac{\sum \frac{A_i}{A_0}}{\sum \frac{A_b}{A_0}}\right)$ and H.

2.4. Calculation of the retention index

The mean sedimentation rate (D_{av}, cm year^{-1}) in a region have the following relationship with the rate of sediment input (Q_S, t year^{-1}) and the rate of sediment escape (Q_E, t year^{-1}), following Gao et al. (2011):

$$D_{av} = 10^5 \times \frac{Q_S - Q_E}{A\gamma}, \tag{5}$$

where A (m^2) is the area of sediment deposition, and γ (kg m^{-3}) is the dry bulk density of the sediment.

Sediment supply for the study area can be attributed to two dominant sources, riverine and shelf-derived sediments. Therefore, Eq. (5) is modified as follows:

$$D_{av} = 10^5 \times \frac{Q_M + Q_L - Q_E}{A\gamma} \tag{6}$$

where Q_L (t year^{-1}) is the riverine sediment discharge rate and Q_M (t year^{-1}) is the shelf-derived sediment discharge rate.

The total amount of sediments supplied to the study area can be linked to the amount of sediments retained there with a concept of sediment retention index (R), which is expressed simply as (Gao, 2007):

$$\begin{aligned} R &= 1 - \frac{Q_E}{Q_M + Q_L} \\ &= \frac{Q_D}{Q_M + Q_L} \end{aligned} \tag{7}$$

where Q_D (t year^{-1}) is the rate of sediment deposition in a given region. Also, a relationship between the sediment retention index and the mean sedimentation rate in a region can be established by combining Eqs. (6) and (7):

$$\begin{aligned} D_{av} &= 10^5 \times \frac{R(Q_M + Q_L)}{A\gamma} \\ &= 10^5 \times \frac{Q_D}{A\gamma}. \end{aligned} \tag{8}$$

Consequently, the following equation can be obtained from Eq. (6):

$$Q_E = Q_M + Q_L - D_{av}A\gamma \times 10^{-5} \tag{9}$$

On the basis of Eqs. (7), (8) and (9), we should know a group of parameters (including A, γ, D_{av}, Q_E, Q_D, Q_M and Q_L) of the study area in order to derive its retention index.

2.4.1. Data of riverine sediment discharge, Q_L

The Changjiang is the primary source of sediment for the study area, whose sediment discharge is taken as the value measured at the Datong hydrological station, the closest station to the river mouth that is free of tidal influence (see Fig. 1a and Table 1).

Other riverine sediment comes from the medium and small rivers along the coasts of Zhejiang, Fujian and west Taiwan (see Fig. 1b). Hydrological data of sediment discharge of these rivers are collected from published papers (see Tables 1 and 2).

2.4.2. Estimation on the shelf-derived sediment supply, Q_M

In this study, spatial ranges of the CSDDM can be defined as the along-shelf muddy deposition in the East China Sea (Qin, 1963; Shi, 2012). Shelf-derived sediment supply from the north, the east and the south should be taken into account.

Modern sediment dynamics in the CSDDM is controlled by ocean circulation, tidal current and river water discharges as well (J.P. Liu et al., 2007; see Fig. 1a). Mud can be kept on the shallow inner-shelf seabed by a dynamic barrier in the vertical due to water-column stratification, which restricts the upward mixing of suspended sediment (Liu et al., 2018). Therefore, suspended sediment exchange along the spatial boundaries between muddy and sandy depositions can be estimated as zero. Correspondingly, shelf-derived sediment supply from the east and the south are supposed to be zero. On the other hand, the northern boundary of the study area may receive sediment carried by the Northern Jiangsu coastal current (NJCC), according to Lin (1988), Liu et al. (2010) and Zhan et al. (2016), which will be discussed further in Sections 3 and 4.

2.4.3. Calculation of the deposition flux, Q_D

A dataset comprising sedimentation rates that fully cover the CSDDM is required to calculate the deposition fluxes in the study area. A uniformly distributed data points will result in a result that is more reliable than other distributions. Here, > 200 data pints of ^{210}Pb and ^{137}Cs dating, from the study area, including those from published papers and unpublished reports/dissertations, from 1980 onwards were collected as a supplement to those obtained in this study. All data were then interpolated using the ordinary Kriging method with circular semivariogram model (see Table 3 for details) provided by the Geostatistical analyst module of ESRI ArcGIS software. In addition, sedimentation rates along the eastern boundary of CSDDM (between sand and mud) were set as 0 cm year^{-1} to diminish unreasonable interpolation results. The output cell size of interpolation is 0.03-degree (≈3.1 km), and the deposition fluxes (Q_D, t year^{-1}) were calculated using the following integral:

$$Q_D = 10^{-5} \times \int A_{grid} \bullet D_{av-grid} \bullet \gamma. \tag{10}$$

where A_{grid} is the area of a cell (about 9.632×10^6 m^2), and $D_{av\text{-}grid}$ (cm year^{-1}) is the sedimentation rate of a cell obtained through interpolation.

The dry bulk density of unconsolidated marine sediment is closely related to the grain size and water content or porosity (Hamilton and Bachman, 1982; Flemming and Delafontaine, 2000; Jia et al., 2003). Although direct measurements of dry bulk density in the study area are surprisingly rare, it could be derived using the following equation, assuming that all the voids within the sediments are filled with seawater:

$$\gamma = (1 - P/100)\rho_s \tag{11}$$

where P is the porosity (unit: %) and ρ_s (kg m^{-3}) is the density of solid sediment. We use 2600 kg m^{-3} for the value of ρ_s.

According to Hamilton and Bachman (1982), porosity and mean grain size are concordant for unconsolidated sediments and fit the following empirical equation:

$$P = 22.01 + 9.24M_Z - 0.365M_Z^2 \tag{12}$$

where M_Z is the mean grain size (unit: ϕ) of the sediments. Data of mean grain size of surficial sediments in the study area are available (Tao, 2011; Shi, 2012; Wang et al., 2016; Gao et al., 2017). Therefore, the corresponding porosity and dry bulk density were calculated using Eqs.

Table 1
Hydrological and sediment data for the major rivers transporting sediment from the continent into the study area.

River	Length (km)	Drainage basin area (km^2)	Runoff ($10^8\ m^3\ year^{-1}$)				Sediment discharge ($10^4\ t\ year^{-1}$)			
			Mean	Maximum	Minimum	Data span	Mean	Maximum	Minimum	Data span
1. Changjiang	6300①	1,800,000①	9114.0①	14,337.0①	7132.0①	1950–1982	47,000.0	67,900.0	34,100.0	1953–1980
2. Qiantangjiang	428①	41,758①	382.7①	698.4①	168.5①	1950–1982	658.7②	1328.0②	132.0②	Before 1985
3. Caoejiang	192①	6046①	44.3①	65.6①	25.6①	1950–1982	128.7②	252.9②	50.6②	Before 1985
4. Yongjiang	131③	4572②	28.6①	51.9①	9.8①	1950–1982	35.9②	–	–	Before 1985
5. Jiaojiang	202③	6591③	65.8①	130.5①	27.2①	1950–1982	123.4②	407.0②	32.0②	Before 1985
6. Oujiang	380③	18,169③	190.0①	307.4①	90.9①	1950–1982	266.5②	635.2②	46.7②	Before 1985
7. Feiyunjiang	195③	3729③	44.6①	72.9①	22.3①	1950–1982	68.7②	249.0②	12.0②	Before 1985
8. Aojiang[a]	82③	1545③	18.3①	31.7①	9.2①	1950–1982	23.7②	–	–	Before 1985
9. Shuibeixi	45④	367④	4.4④	7.8④	2.5④	1963–1979	7.3④	17.5④	2.1④	1965–1979
10. Jiaoxi	165④	5638④	65.7④	101.0④	37.9④	1951–1979	107. 0④	248.0④	20.2④	1955–1979
11. Huotongxi	126④	2264④	27.2④	43.2④	14.0④	1958–1979	34.5④	65.1④	7.2④	1959–1972[c]
12. Aojiang[b]	137④	2655④	30.2④	44.4④	16.4④	1958–1979	44.7④	70.8④	14.4④	1959–1966
13. Dazhangxi	191④	4034④	40.3④	62.7④	23.6④	1951–1979	55.6④	192.0④	18.9④	1951–1979
14. Minjiang	541④	60,992④	600.0④	903.0④	309.0④	1950–1979	829.0④	2131.0④	319.0④	1951–1979
15. Mulanxi	105④	1732④	15.6④	27.2④	7.4④	1950–1979[c]	46.8④	147.0④	13.5④	1959–1979
16. Jinjiang	182④	5275④	50.9④	87.7④	29.3④	1950–1979[c]	223.0④	447.0④	79.9④	1951–1979[c]
17. Jiulongjiang (Xixi)	139④	3419④	37.0④	61.3④	20.7④	1951–1979	77.7④	183.0④	21.3④	1952–1979[c]
18. Jiulongjiang (Beixi)	285④	14,741④	148.0④	238.0④	99.6④	1950–1979	307.0④	748.0④	114.0④	1952–1979[c]
19. Zhangjiang	58④	961④	10.3④	17.4④	6.0④	1956–1979[c]	39.1④	78.9④	10.4④	1960–1979[c]
20. Zhaoan Dongxi	93④	1150④	11.9④	18.7④	5.7④	1956–1979[c]	39.4④	66.1④	19.9④	1965–1979[c]

Data sources: ① Lin and Chu (1984); ② Dai (1988); ③ ZJSMG (2010); ④ Lin (1990).
[a] In Zhejiang Province.
[b] In Fujian Province.
[c] No data were recorded for some of the years.

Table 2
Mean annual sediment discharge of rivers emptying into the Taiwan Strait. After Huh et al. (2011).

River	Drainage basin area (km^2)	Sediment discharge ($Mt\ year^{-1}$)	Data span
1. Tanshui	2726	11.45	1949–1990
2. Touchien	566	2.56	1949–1990
3. Houlong	537	4.37	1949–1990
4. Taan	758	4.94	1949–1990
5. Tachia	1236	4.03	1949–1990
6. Wu	2026	6.79	1949–1990
7. Choshui	3157	63.87	1949–1990
8. Peikang	645	2.35	1949–1990
9. Potzu	427	0.83	1949–1990
10. Pachang	475	3.16	1949–1990
11. Chishui	379	2.06	1949–1990
12. Tsengwen	1177	31.00	1949–1990

Twelve rivers are listed here following Liu et al. (2006), and their total sediment discharge is 137 $Mt\ year^{-1}$.

Table 3
Parameters and prediction errors for the Kriging method used in this study.

Category	Parameters	Option/values
Interpolation methods	Kriging	Ordinary
	Semivariogram model	Circular
	Nugget	0.493 (by default)
	Lag size	0.425
	Number of lags	12
	Output cell size	0.030 (degree)
Prediction errors	Root-Mean-Square	0.690
	Mean standardized	0.012
	Root-Mean-Square standardized	0.943
	Average standard error	0.730

(12) and (11), respectively.

2.4.4. Derivation of the retention index and other parameters

In this study, the area of sediment deposition is considered for three parts of the CSDDM. The reason of dividing the study area is to understand its spatial diversity in terms of along-shelf budgeting patterns of input, storage, bypass, and final accumulation of sediments. The spatial scope of the provincial administrative region (including both land and sea) is another important consideration when dividing the study area into sub-regions, as it is easy to merge data of riverine sediment discharges and to divide the sea waters. Here, three sub-regions were identified: the Changjiang subaqueous delta region (CJM), the Zhejiang coastal mud region (ZJM), and the Fujian coastal mud region (FJM).

Suspended sediment is transported southward within the CSDDM, ending at the middle of the Taiwan Strait (J.P. Liu et al., 2007; Liu et al., 2018). The budgeting patterns of this along-shelf system can be investigated from the south to the north. As discussed in Section 2.4.2, the amount of sediment escaping from the FJM is assumed to be zero, and supply of shelf-derived sediment from the outer-shelf is negligible. Therefore, $Q_{E\text{-}FJ}$ in Eq. (9) is assigned with zero for the FJM. In addition, the riverine sediment supply ($Q_{L\text{-}FJ}$) of the FJM was obtained from hydrological data (see Tables 1 and 2), the sedimentation rate ($D_{av\text{-}FJ}$) over the last 100 years was derived by interpolation (see Section 2.4.2 for details), and the area (A_{FJ}) was calculated with ESRI ArcGIS software. Finally, the shelf-derived sediment supply ($Q_{M\text{-}FJ}$) of FJM was calculated using Eq. (9), which is equivalent to the rate of sediment escape from ZJM ($Q_{E\text{-}ZJ}$). In such a way, the rates of input, retention and bypass, together with the retention index, were calculated for the three sub-regions (i.e., CJM, ZJM and FJM).

3. Results

3.1. Sediment supply (Q_L, Q_M)

The mean values of the Changjiang sediment discharge over 30 years (1953–1980) and 60 years (1953–2010) are 470 and 390 $Mt\ year^{-1}$, respectively (MWR 2000–2016), with the annual sediment discharge decreasing in a stepwise trend (Dai et al., 2007; Gao et al., 2015b). The annual mean sediment discharge decreased to 140 $Mt\ year^{-1}$ after the Three Gorges Dam was built in 2003 (MWR 2000–2016; see Fig. 2).

The total sediment discharge from the Zhejiang coastal rivers is

~15 Mt year^{-1}, of which seven of the major rivers contribute ~13 Mt year^{-1} (Dai, 1988; Table 1). The sediment delivery from Fujian province is also derived from local rivers, with the total discharge being ~20 Mt year^{-1}, of which 12 major rivers contribute~17 Mt year^{-1} (Lin, 1990; Table 1).

Lin (1988) employed a whole-sample approach comprising end-member analysis of all grain sizes, and a mineral-tracer method combining heavy minerals with sand and silt, and clay minerals with fine particles to investigate the source-to-sink pattern of the CJM. He proposed that annual sediment supply by NJCC to CJM is estimated ~70 Mt year^{-1}, of which ~58 Mt year^{-1} is silt and clay (Lin, 1988).

The southern boundary of the study area receives sediments discharged from west Taiwan rivers. The magnitude of this input is 60–150 Mt year^{-1} (Kao and Milliman, 2008; Liu et al., 2008; Xu et al., 2009; Huh et al., 2011; Table 2), varying annually and inter-annually due to the variability of extreme events such as typhoons. However, a considerable portion of these sediments consists of coarse particles and are deposited near the river mouths; much of the finer-grained sediment is believed to escape either southward into the South China Sea or northeastward into the Okinawa Trough (Liu et al., 2008; Xu et al., 2009). Therefore, a sediment flux of 70 Mt year^{-1} is adopted in this study to represent the riverine sediment discharge from western Taiwan, in accordance with Xu et al. (2009).

According to the above estimations, the total sediment supplied to the study area is ~535–725 Mt year^{-1}. Assuming a mean value of 645 Mt year^{-1}, the sediment discharge from the southern Yellow Sea, the Changjiang, Zhejiang, Fujian and Taiwan coastal rivers are 70, 470, 15, 20, and 70 Mt year^{-1}, respectively.

3.2. Deposition fluxes and retention indices (Q_D, R)

The sedimentation rates in the study area show significant spatial trends, decreasing steadily from the north towards the south, and from the shoreline towards the open sea (Fig. 3). The highest sedimentation rate appears in CJM, exceeding 4 cm year^{-1}. The estimated sedimentation rates are 1–2, < 1.5, and < 0.5 cm year^{-1} for the Zhejiang coast, the Fujian coast, and the eastern boundary of the study area, respectively. The areas of high sedimentation rates (i.e., the Changjiang Subaqueous Delta and the inner-shelf off the Zhejiang coast) are consistent with the maximum thickness of Holocene deposition reported by J.P. Liu et al. (2007).

Tao (2011) collected hundreds of mean grain size and porosity data points from the modern shelf sediments (including surficial sediment and short cores) and found that Eq. (12) is applicable in the East China Sea in the case that M_z is finer than 1 ϕ (Fig. 4). The porosity derived with Eq. (12) is also consistent with the results obtained by Wang et al. (2016), who presented data of mobile mud samples in the East China Sea with a porosity of 0.50–0.75 (Fig. 4). The M_z values of surficial sediments in the study area are mainly between 5 and 8 ϕ (Shi, 2012; Wang et al., 2016; Gao et al., 2017). Hence, the dry bulk density of inner-shelf sediments in the East China Sea is estimated to be between 700 and 1000 kg m^{-3} (Table 4).

Table 4
Calculation of the dry bulk density of surficial sediments on the inner-shelf of the East China Sea.

Mean grain-size (ϕ)	Porosity	Solid sediment density (kg m^{-3})	Dry bulk density (kg m^{-3})
5.0	59.1	2600	1064
5.5	61.8	2600	993
6.0	64.3	2600	928
6.5	66.6	2600	867
7.0	68.8	2600	811
7.5	70.8	2600	760
8.0	72.6	2600	713

Note: The mean grain size is based on Shi (2012, p. 246), Wang et al. (2016) and Gao et al. (2017), and the corresponding porosity and dry bulk density can be derived using Eqs. (12) and (11), respectively.

Flemming and Delafontaine (2000) provided another approach to determine the value of dry bulk density using mud contents. The surficial sediment in the study area is composed mainly of silty clay, clayey silt, and silt, with a mud content of 70%–90% (Shi, 2012; Wang et al., 2016; Gao et al., 2017). Consequently, the dry bulk density is inferred to be 400–800 kg m^{-3} (Fig. 5).

DeMaster et al. (1985) used a value of 700 kg m^{-3} for dry bulk density to estimate the deposition flux in the CJM. This study used the same value with reasonable variations, 700 ± 300 kg m^{-3}, which is consistent with the results of Hamilton and Bachman (1982) and Flemming and Delafontaine (2000). Thus, the annual mean deposition flux of the study area over the last century is estimated at ~683 ± 293 Mt year^{-1} (390–976 Mt year^{-1}). This value is close to that of the sediment supply (i.e., 645 Mt year^{-1}, ranging from 535 to 725 Mt year^{-1}).

Recently, Qiao et al. (2017) estimated that the burial sediment in the East China Sea mud area is totally 794 Mt year^{-1}. This amount would be only 14% less than the mean value our estimation, if the number of 700 kg m^{-3} instead of 950 kg m^{-3} had been adopted by Qiao et al. (2017) as the dry bulk density of surficial sediment.

The area of CJM is 1.265 × 10^4 km^2, and its deposition flux is 190 ± 80 Mt year^{-1} (Fig. 6). Our results are consistent with the values

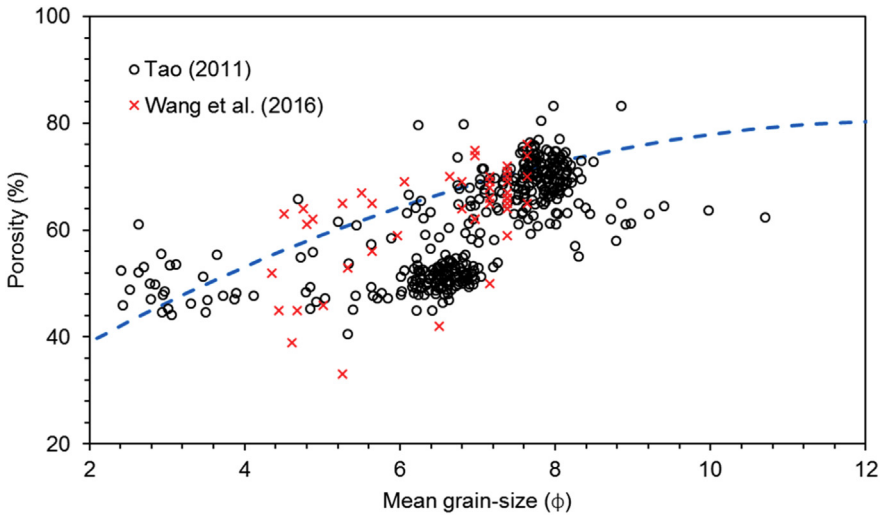

Fig. 4. Measured data showing mean grain size versus porosity of sediments sampled in the East China Sea. The blue dashed line is the empirical relationship given by Hamilton and Bachman (1982), as shown in Eq. (12) in this paper. (For interpretation of the references to colour in this figure legend, the reader is referred to the web version of this article.)

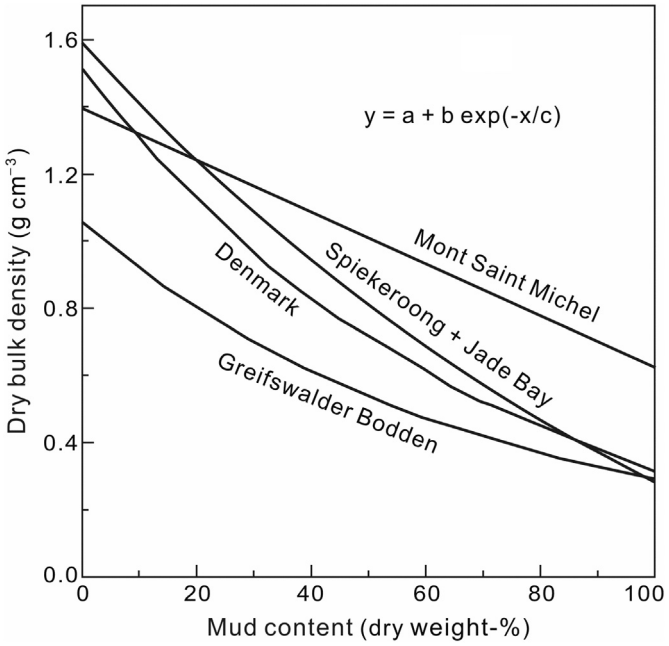

Fig. 5. Relationship between mud content and dry bulk density of surficial sediments on tidal flats.
(After Flemming and Delafontaine (2000).)

estimated by DeMaster et al. (1985) (1.0×10^4 km^2 and 200 Mt year^{-1}). The area of the ZJM is 4.784×10^4 km^2, and the deposition flux within this region is 350 ± 150 Mt year^{-1}. This latter value far exceeds the values presented in previous studies (Milliman et al., 1985; Jin, 1992; Gu et al., 1997). The area of FJM is similar to that of ZJM, but the deposition flux is only 150 ± 63 Mt year^{-1} (Fig. 6), which is consistent with the annual mean deposition flux of 160 Mt year^{-1} in the same area calculated by Huh et al. (2011). Shelf-derived sediment from ZJM constitutes approximately one-third of the total input for FJM. The remaining sediment supplied to the FJM comes from the coastal rivers of Fujian and west Taiwan.

The ratio of net deposition within the CJM, ZJM, and FJM is ~3:5:2 (Table 5). The sediment retention indices of the three sub-regions are 0.35, 0.86, and 1.00 (Table 5). The estimated retention index of CJM (0.35) is lower than that obtained by the China-US joint survey (i.e., 0.40).

4. Discussion

4.1. Mass balance between source and sink for CSDDM

In terms of the sediment balance of CSDDM over the last century, the hydrological data of sediment discharge in mainland China are only available for the last 30 to 60 years. Therefore, uncertainties exist regarding the values used to represent sediment discharge over the past 100 years. Further, the estimation of deposition fluxes is no more accurate than observations of the sediment discharge of rivers. Two main factors affect the estimations: the value of dry bulk density of the surface sediment and the reliability of the interpolation of sedimentation rates.

4.1.1. Is the mean annual sediment supply flux representative?

Wang et al. (2008) used the rating curve method to extrapolate the time series data at Datong and inferred that the sediment discharge between 1865 and 1952 was 488 Mt year^{-1}. This result is consistent with other estimated sediment discharge values based on different approaches (Milliman and Syvitski, 1992; Syvitski and Morehead, 1999). If combined with measured data, the annual sediment discharge at Datong between 1865 and 2010 is ~450 Mt year^{-1}. This number is close to the value used in this study, 470 Mt year^{-1}; i.e., the 30-year (1950–1980) mean value of sediment discharge measured at Datong. In addition, the riverine sediment discharge from Zhejiang and Fujian provinces, as used in this study, is also based on the measured hydrological data during the same 30-year period (Table 1). Therefore, the sediment supply flux of the mainland rivers adopted in this study is consistent for all rivers in terms of timescale and values used.

Up to now, sediment discharge and retention in the 650 km lower river section between Datong and river mouth keep unknown. According to Wang et al. (2009) and Gao et al. (2015b), this river section experienced an obvious switch from sedimentation to erosion around 1985 due to upstream dam construction. This switch might indicate that the sedimentation and erosion in the lower river section balance each other over the last century, which does not diminish the significance of 470 Mt year^{-1} as the mean sediment discharge of the Changjiang adopted in this research. In the future, we should consider the sediment retention in the lower river section.

The medium and small rivers in Zhejiang and Fujian provinces have also experienced a decrease in sediment discharge due to human activities (Dai et al., 2007; C. Liu et al., 2007; Song et al., 2012; Fig. 7). For example, the mean sediment discharges for the largest three coastal rivers in Zhejiang and Fujian provinces, the Qiangtangjiang, the Oujiang and the Minjiang Rivers, are 317 (1977–2015), 195 (1956–1998) and 546 Mt year^{-1} (1950–2015), respectively. A quarter to a half reduction in sediment discharge may have occurred in these rivers when compared with the hydrologic data collected before 1985 (Table 1). The total decrease in sediment discharge for the mainland coastal rivers is ~10 Mt year^{-1}, < 10% of the sediment discharge decrease of the Changjiang.

To date, no direct observation of sediment transport between the southern Yellow Sea and the Changjiang Estuary has been reported. Fortunately, there are circumstantial evidences that could provide some clues on this issue. Firstly, the year-round North Jiangsu Coast Current (NJCC, see Fig. 1a) is possibly an effective carrier of suspended sediment. It flows southward along the Yellow Sea coast at a mean velocity of ~10 cm s^{-1}, roughly following the 30–40 m isobaths (Qiao, 2012). Suspended sediment transported by NJCC may deposit to the east of 30 m isobaths out of the Changjiang North-branch, where fast deposition rates were observed in this study (see Fig. 3) and by Zhan et al. (2016). The recent work by Wu et al. (2018) showed that an up-shelf transport persists in the inner southwestern Yellow Sea, indicating the Changjiang Estuary could be a source area for the inner southwestern Yellow Sea with water depth < 15–20 m. However, Wu et al. (2018) studied the water transport (residual current) only; therefore, net sediment transport in this shallow waters (< 15–20 m) is still unknown. Secondly, numerical modeling performed by Xing et al. (2012) showed that net transport of suspended sediment from the southern Yellow Sea to the Changjiang Estuary is significant in both winter and summer. Thirdly, Yu et al. (2014) reported a southward net sediment flux along the west coast of the southern Yellow Sea in winter, and the magnitude of the flux is estimated as 46.0×10^4 t day^{-1} during spring tides. Lin (1988) proposed that the sediment transport rate from the southern Yellow Sea to the Changjiang Estuary region is 70 Mt year^{-1}. This result is semi-quantitative and reasonable.

Previous studies have calculated the sediment discharges of west Taiwan rivers (Kao and Milliman, 2008; Liu et al., 2008; Huh et al., 2011); hence, the results are not repeated here.

The annual mean sediment discharge of the whole study area, as estimated in Section 3.1, is within an acceptable range of variation, as the difference between the minimum (535 Mt year^{-1}) and maximum (725 Mt year^{-1}) values is 26%.

4.1.2. Reliability assessment of the interpolation of sedimentation rates

The study area generally experiences sediment accumulation. Nonetheless, it is unlikely that net accretion occurs simultaneously

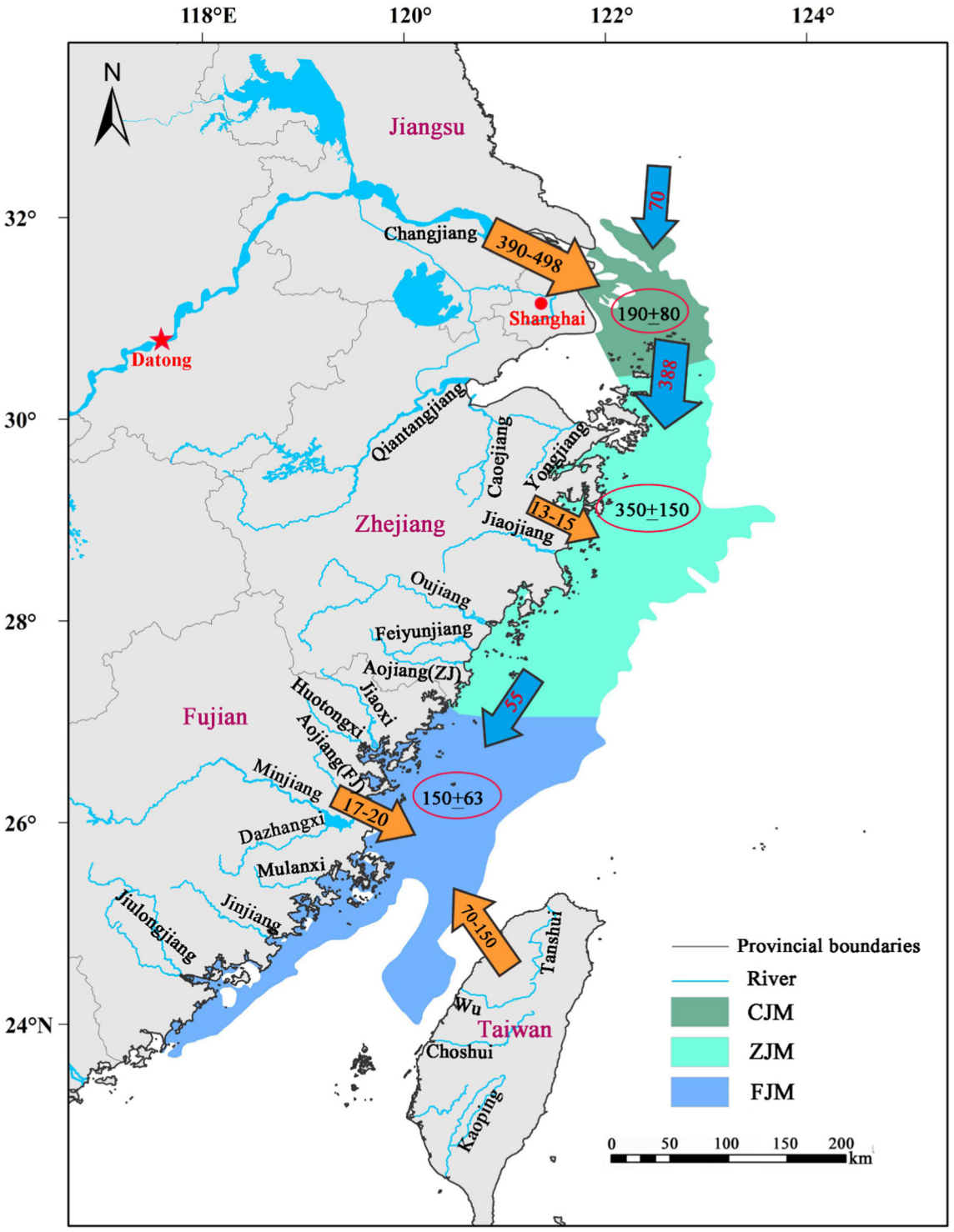

Fig. 6. Summary of sediment input, deposition, and output in the CJM, ZJM, and FJM (units: Mt year^{-1}). Brown arrows indicate riverine sediment input, blue arrows indicate shelf-derived input, and red circles indicate deposition fluxes. (For interpretation of the references to colour in this figure legend, the reader is referred to the web version of this article.)

everywhere. All the short cores presented in published papers contain information on sedimentation rates, but some are less reliable. The obtained total deposition fluxes are representative only if less reliable data are eliminated. Based on this argument, using the reliable data only to interpolate sedimentation rates will likely increase the reliability of the total deposition fluxes in the study area. However, the data that should be excluded remain unknown because the identity of the less reliable cores is not known.

The kriging interpolation method is used to produce a trend of sedimentation rates based on the spatial distribution of the data points, with high values suppressed. The total number of data points used is 246, and the mean and standard deviation of the sedimentation rates are 1.40 ± 1.23 cm year^{-1} for the collected datasets and 1.38 ± 0.88 cm year^{-1} for the interpolated datasets. Comparing the collected sedimentation rate with the corresponding interpolated rate leads to the following conclusions.

Table 5
Sedimentation rates and retention indices for the sub-regions.

Sub-region	A $\times 10^4$ km^2	D_{av} cm year^{-1}	Q_D Mt year^{-1}	Q_L Mt year^{-1}	Q_M Mt year^{-1}	Q_E Mt year^{-1}	R
CJM	1.265	2.15	190.0	470.0	70.0	387.7	0.35
ZJM	4.784	1.04	347.9	15.0	387.7	54.8	0.86
FJM	4.303	0.48	144.8	90.0	54.8	0.0	1.00

Note: 'A' is the area of a sub-region, D_{av} is the mean deposition rate over the sub-region, Q_D is the deposition flux in each sub-region, Q_L is the riverine sediment discharge rate into a sub-region, Q_M is the shelf-derived sediment discharge rate into a sub-region, Q_E is the rate of sediment export from a sub-region, and R is the retention index. The dry bulk density is taken as 700 kg m^{-3}.

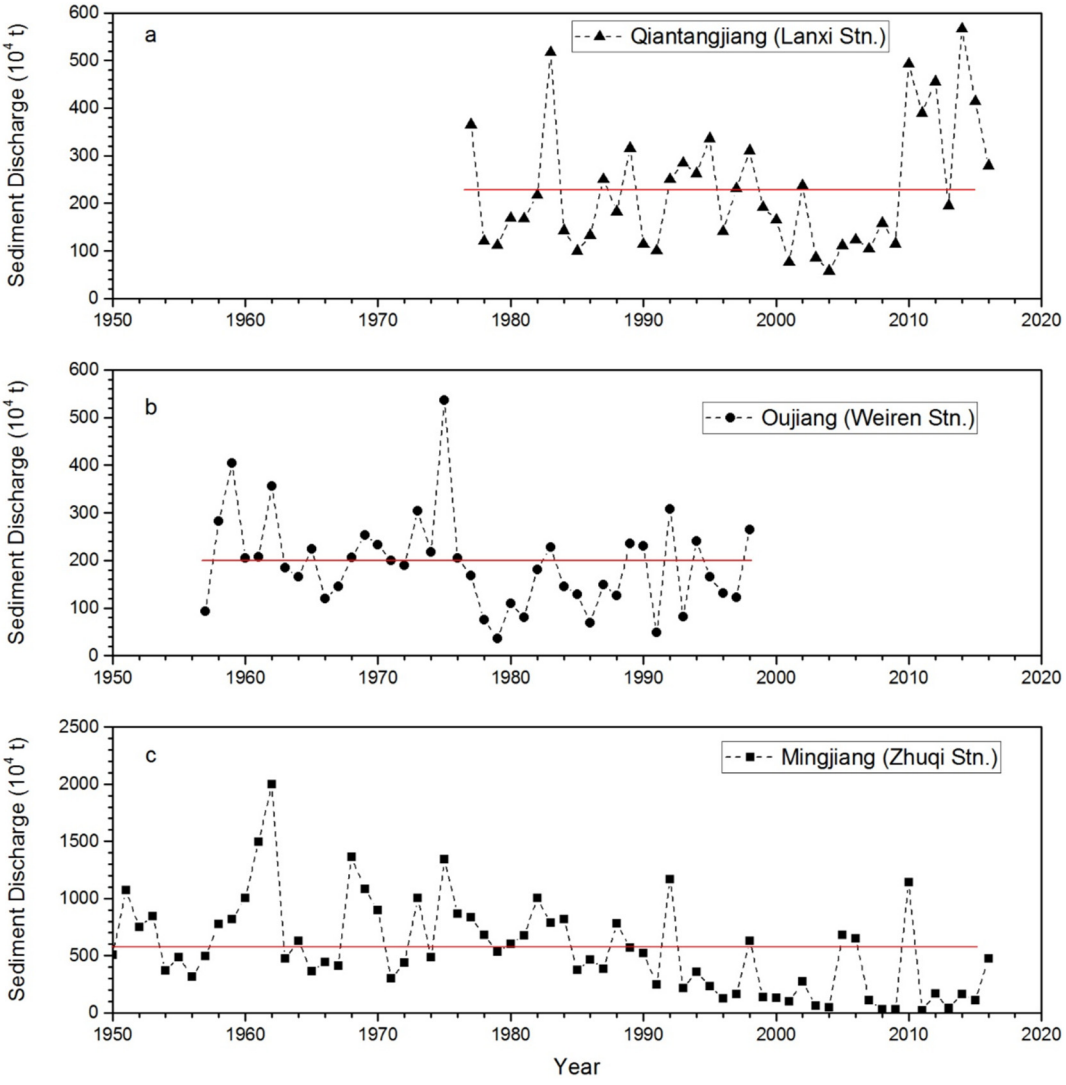

Fig. 7. Annual sediment discharge measured at the (a) Lanxi (Qiantangjiang R., 1977–2016), (b) Weiren (Oujiang R., 1956–1998), and (c) Zhuqi (Minjiang R., 1950–2016) stations. The red line on each chart illustrates the corresponding mean sediment discharge. (For interpretation of the references to colour in this figure legend, the reader is referred to the web version of this article.)
Data sources: Qiantangjiang R. and Minjiang R. are according to MWR (2000–2016), and Oujiang R. is after Song et al. (2012).

(1) The mean values (1.40 ± 1.23 cm year^{-1} VS 1.38 ± 0.88 cm year^{-1}) are similar, which indicates that the interpolated result and the original data are almost identical. The scatter among the original data is larger than that among the interpolated values.
(2) For sedimentation rates of < 2.63 cm year^{-1} (i.e., the mean plus 1 standard deviation), the linear regression equation relating the interpolation result to the original data is close to y = x (Fig. 8). These samples constitute ~84.5% of the collected datasets.
(3) For sedimentation rates of > 2.63 cm year^{-1}, the interpolation result is significantly less than the measured value. On average, the mean interpolated values are ~75% of the collected values. These samples comprise 15.5% of the total dataset.

Statistical analysis indicates that the sedimentation rates obtained by kriging interpolation match the collected samples for most of the data points (84.5%). For stations with high sedimentation rates (> 2.63 cm year^{-1}), the interpolation has a peak-eliminating effect,

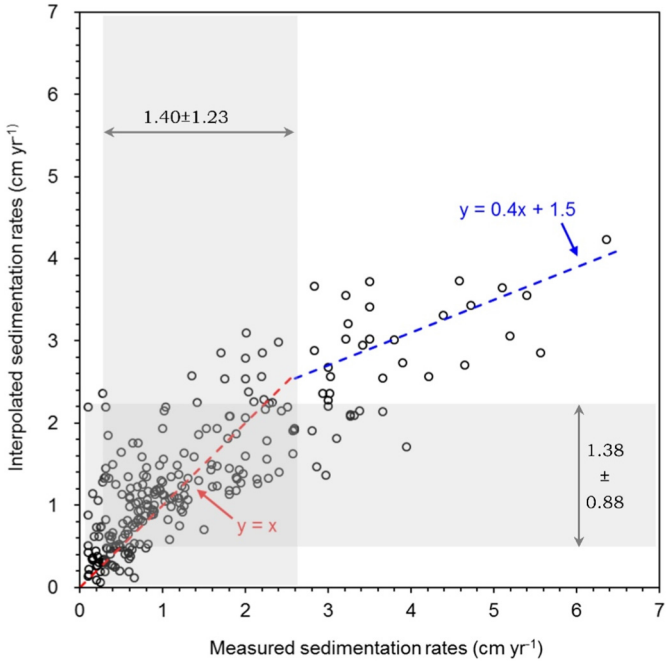

Fig. 8. Measured sedimentation rates versus values estimated using the kriging interpolation method. The vertical and horizontal gray bars illustrate the mean value ± 1 standard deviation.

and the reduction is ~25%. Therefore, kriging interpolation has reduced the peaks associated with the unreliable data to some degree.

4.2. Sediment budgets and flux balance in ZJM and FJM

Approximately 30 years ago, a detailed investigation of the sedimentary dynamics of the Changjiang Estuary was conducted by China and the United States (Milliman and Yang, 2014). This investigation included the first quantitative study of the retention index of the sediment in the Changjiang Delta and proposed that ~40% of the sediment carried by the Changjiang was deposited within the subaqueous delta (DeMaster et al., 1985), and ~30% of the Changjiang sediment that flowed into the sea escaped to the south and entered the ZJM and FJM (Milliman et al., 1985). Unfortunately, Milliman et al. (1985) did not clearly explain the destination of the remaining 30% of the sediment. This proposition was fundamental and groundbreaking, and many subsequent studies have confirmed this view (Jin, 1992; Gu et al., 1997). However, several aspects of these early studies can be improved upon.

Firstly, these early researchers did not consider the possibility that the NJCC supplies sediment to the Changjiang estuary. Therefore, because the total amount of sediment in a closed system must equal 100%, they naturally inferred that 20%–30% of the sediment from the Changjiang escaped to the outer-shelf. Secondly, the total amount of sediment supplied to the ZJM was not in balance with the sediments deposited within it, if the along-shelf distribution pattern proposed by Milliman et al. (1985) were true.

The second problem has already garnered some attentions. For example, by comparing marine charts, Dai (1988) found that near-shore annual sedimentation on the landward side of the 10-m isobaths along the Zhejiang coast is ~100 Mt and estimated that the total annual deposition on the inner-shelf of the Zhejiang coast is ~200 Mt Therefore, the portion of Changjiang sediment transported southward (20%–30%) does not balance the deposition within the ZJM. Dai (1988) suggested that the outer-shelf of the East China Sea represents another important source of sediment supplied to the ZJM. In fact, relict sandy sediments are widely distributed outside the ZJM and FJM. Thus, it is not reasonable to conclude that these sandy relict areas contributed fine-grained sediment to the Zhejiang coast. Similarly, Su and Huh (2002) studied the modern sediment balance throughout the East China Sea, and found that sediment supply to the East China Sea has a deficiency of > 540 Mt year^{-1}. They proposed that the mass transported from the southern Yellow Sea to the East China Sea is far greater than previous estimates. A recent study supports the speculation of Su and Huh (2002). Qiao et al. (2017) inferred that fine sediment from the Yellow Sea (and from coastal erosion and re-suspension of sediments from other areas) contribute totally ~238.3 Mt year^{-1} to the mud deposition over the East China Sea.

The above studies suggest that the imbalance between deposition and supply in the East China Sea was a persistent problem noted by many researchers. Considered attentions should be focused on identifying the sediment sources from the Yellow Sea to the East China Sea rather than the potential supply of relict sediments from the outer-shelf to the inner-shelf muds.

The results of this study provide a positive answer to the question raised by Dai (1988); i.e., whether the sediment supplied to the inner-shelf in Zhejiang coastal sea can balance with the deposition in the ZJM. The deposition of modern sediment supplied by continental rivers is controlled by the dynamic environment of the East China Sea and thereby limited in the inner-shelf muds (Liu et al., 2006; Liu et al., 2018). We find that sediment supplied by the Changjiang, coastal rivers in Zhejiang, Fujian and western Taiwan, and the NJCC account for the observed deposition within the CSDDM over the past century. Therefore, a surplus of sediment available to be transported directly across the continental shelf to the outer sea may not exist. Actually, < 5% of the fluvial sediment discharging into the East China Sea could escape the shelf edge (Qiao et al., 2017).

Our study relies on two assumptions. Firstly, the sediment carried by ZFCC cannot travel through the Taiwan Strait to the South China Sea; i.e., $Q_{E\text{-}FJ}$ is 0. Secondly, the transport of sediment supplied by western Taiwan rivers and carried by the Taiwan Current are limited, terminating at the offshore boundary of Zhejiang and Fujian provinces. Ruan et al. (2012) found that the distribution of suspended particle-size end-members indicates a pathway for fine particles sourced from the west coast of Taiwan to enter the East China Sea, rather than being transported through the Taiwan Strait to enter the South China Sea. Support for the second assumption is obtained from the perspective of mineral assemblages and grain size distributions. The northern boundary of the sandy sediment transport from the west coast of Taiwan lies at ~27°N; thus, sediment from Taiwan does not extend into the sea off the Zhejiang coast (Xu et al., 2009). The clay mineral compositions of the Changjiang sediments differ significantly from those of the coastal rivers in western Taiwan (Xu et al., 2009, 2012; Li et al., 2012). Studies have also shown that a Changjiang-type clay mineral assemblage dominates as far south as 26°N (Xu et al., 2009; Zhou et al., 2003).

4.3. Retention indices at different time scales

Gao (2010) noted that the mean sedimentation rate of a subaqueous delta is affected by both the river sediment discharge and the sediment retention index (see Eq. (5)), where the sediment retention index is a variable that is independent of river sediment discharge. Therefore, the sediment retention index varies over different timescales.

Based on sedimentary analysis of 265 cores, Li et al. (2003) calculated the total amount of sediment accumulated in the Changjiang Delta during the postglacial cycle (after the Last Glacial Maximum) to be 1.77×10^6 Mt. They also inferred that in the same period, the sediment discharge of the Changjiang and the sediments delivered to adjacent coastal seas were on average 236–486 and 118–354 Mt year^{-1}, respectively. We can deduce that the retention index value of the Changjiang Delta during the postglacial period was between 0.27 and 0.5.

On millennial to Holocene timescales, J.P. Liu et al. (2007) proposed that during the past 7000 years the amount of sediments deposited in the Changjiang Delta and in its distal muds (ZJM and FJM) are 1.16×10^6 Mt and 0.54×10^6 Mt, respectively, while the total is 1.7×10^6 Mt It is inferred that for the past 7000 years, the retention index of the Changjiang Delta is 0.68, and the sediment discharge in the ZJM and FJM constituted 32% of the total sediment transported by the Changjiang into the sea. During this period, the retention index of the Changjiang Delta was higher than the average of the past 15,000 years because a large amount of sediment was involved in the construction of the subaerial delta (Chen et al., 1979; Gao and Collins, 2014). In addition, the Changjiang was not turbid until the early twelfth century (Lin and Pan, 2005). These finding may indicate that the amount of sediment escaping to the sea was not significant at that time.

Many researchers have used the results of the China-US joint Changjiang Estuary survey (DeMaster et al., 1985) to calculate the retention index on a century scale. Our study found that the retention index of the CJM (0.35) is less than that of the China-US joint survey (0.40). The difference in retention index value arose because previous studies did not consider sediment sources other than the Changjiang for the CJM, meaning that only the Q_L term was considered. Conversely, the contribution of the NJCC was considered in this study, meaning that the Q_M term was considered. Therefore, according to Eq. (7), although $Q_{S\text{-}CJ}$ is similar to the data adopted by DeMaster et al. (1985), the resulting value of R is smaller.

4.4. The land-coast-shelf system behavior

4.4.1. A lesson learned from the Old Huanghe (Yellow River) Delta

The Old Huanghe Delta, 350 km northwest of the Changjiang estuary, presents a situation that is similar to, but more severe than that of the modern Changjiang Delta. The Old Huanghe channel entered the south Yellow Sea from 1128 CE to 1855, and added an area of 9000 km^2 to the continent. The river mouth extended 90 km seawards and formed a subaqueous delta with an area of 2.5×10^4 km^2. The total amount of sediment deposited on the subaerial delta and the subaqueous delta was $\sim 1500 \times 10^8$ t, and the subaerial and subaqueous delta each received half this amount (Li, 1991). After 1855 CE, the Huanghe turned to the north, entered the Bohai Sea, and left the Old Huanghe delta in the northern Jiangsu. The coast subsequently began to adjust, and the erosional recession rate at the most prominent position of the Old Huanghe Delta decreased from 1000 m $year^{-1}$in the 19th century to 100 m $year^{-1}$ in the 1980s. Currently, the coast is mostly stable due to coast-protection projects (Zhang, 1984).

The distance from the Old Huanghe Delta to the Changjiang Estuary is approximately half the distance from the Changjiang Estuary to the middle of the Taiwan Strait. The Old Huanghe Delta has equivalent spatial dimensions to the CSDDM. Furthermore, sedimentary evidence supports a source-to-sink pattern linking the Old Huanghe Delta and CJM. Liu et al. (2010) recovered a long core in CJM to retrieve sediment provenance changes and environmental evolution during the post-glacial period. They found that the uppermost depositional units, characterized by a near-shore environment during the last ~540 years, higher sedimentation rates than underlying units and more influence from the Yellow River in terms of sediment composition, can be logically linked to the period when the Old Huanghe discharged into the South Yellow Sea. Therefore, the future evolution of the CSDDM could be understood by learning stories of the Old Huanghe.

Studies have shown that the critical amount of sediment required to maintain the equilibrium of the Changjiang Delta is ~300 Mt $year^{-1}$ (Yang et al., 2003; Gao, 2007). So far, annual sediment discharge of the Changjiang is much less than the required value. Net erosions have been observed in the CJM since 2007 (Li et al., 2015). In spite of this, the Changjiang will continue to supply > 100 Mt of sediment to the estuary each year (Yang et al., 2011). Adding the ~70 Mt $year^{-1}$ of sediment brought in by the NJCC, the sediment supplied to the CJM will be maintained at ~200 Mt $year^{-1}$ for a long time. The connection of the sediment source to the delta is more robust in the CJM than in the Old Huanghe delta. Accordingly, the erosion in the CJM is expected to be much slower than the rapid erosional recession of the Old Huanghe delta, where the main tributary was disconnected from the delta. In addition, Shanghai and Nantong have already completed seawall protection projects for reclamation and tide protection; these projects will ensure the stability of the coast.

The sediment dynamics of the ZJM are characterized by active deposition taking place in winter (Liu et al., 2018). Re-suspension due to winter monsoon waves and the southward ZFCC supplies additional sediment, but the total amount is less than it was in 1980s. Therefore, the overall sedimentation rate will decrease in the ZJM from an average of 10^0 to 10^{-1} cm $year^{-1}$. However, the deposition in the bays and intertidal zones of the Zhejiang coast may not decrease significantly during the lifetime of man-made projects (50–100 years). Conversely, bays and intertidal zones act as sediment traps in the ZJM. Every summer and fall, five or six typhoons redistribute the muddy sediment on the inner-shelf and cause rapid deposition in local regions near the shoreline (Xie et al., 2001). Also, human activities (such as dredging, reclamation and bottom trawling) may re-distribute the muddy sediment on the inner-shelf, which has to be considered in the future prediction.

For the sub-region FJM, the Changjiang is a secondary source of sediment. It can be inferred that the decrease of the Changjiang sediment discharge will have smaller effect than that within ZJM. On the other hand, due to the global climate change which may enhance climate extreme events, the sediment erosion and transport from Taiwan Island could be further intensified, supplying more sediment to FJM. Therefore, a systematic change for FJM will show a greater temporal lag than that for ZJM, or maintain its present status.

4.4.2. The uniqueness of CSDDM as a mega-delta

Today, anthropologic activities are fundamentally changing deltas globally in two ways: reducing aggradation and accelerating compaction (Syvitski et al., 2009). The recent evolution of the Changjiang system is an example of human activities that are ubiquitous and constituting the main force affecting the morphological evolution. Similar changes were also observed among other large river systems (Syvitski and Saito, 2007; Milliman and Farnsworth, 2011; Xing et al., 2014). Artificial riverbanks and seawalls in the delta prevent further increase in ground elevation, where accretion used to occur via fluvial sedimentation during flood seasons. Dam construction in the Changjiang catchment caused a dramatic reduction in sediment discharge, threatening the stability of the Changjiang Delta front (Yang et al., 2011). These changes are occurring rapidly, within human lifetimes (century-scale).

The CSDDM is unique in two aspects. First, Shanghai, the largest city in China, whose downtown is located only 20–50 km from the sea, is a typical example of high population density and economic activity, and a managed retreat from rising sea level is not an option for Shanghai. Second, the sustainability of the coastal zone of Shanghai, and Zhejiang and Fujian Provinces is physically dependent on the Changjiang Delta. It is the Changjiang-derived sediment that produces the extensive delta system, which has enabled coastal reclamation over at least the past 1000 years (Xu and Zhou, 2004). According to Xu (2000), up to 62% of Shanghai's land has been created by reclamation in the past 2000 years. Parts of the coastline in Zhejiang Province have advanced seawards for tens of kilometers in recent centuries, and 40%–50% of the cultivated land in some coastal counties is reclaimed (Xu and Zhou, 2004). Thus, understanding the dynamics and processes of the Changjiang Delta and along-shelf sediment redistribution will contribute to our understanding of land-coast-shelf system behavior, and will aid in strategic assessment and flexible land management.

5. Conclusions

The amount of sediment supplied to the CSDDM is ~645 Mt year^{-1} on average (535–725 Mt year^{-1}). The amount of sediment deposited in the CSDDM is ~683 ± 293 Mt year^{-1}. The size of supply and deposition of sediments in the study area are approximately balanced, although a large uncertainty also exists in the estimations. On a century scale, the sediment retention index values of the CJM, ZJM and FJM sub-regions are 0.35, 0.86, and 1.00, respectively.

The Changjiang Delta system faces future systemic changes mainly due to reduction in riverine sediment discharge. Net erosion instead of aggradation occurs in the CJM already. The supply of sediment and the sedimentation rates in ZJM and FJM may also decrease accordingly. However, this effect may decrease from the north to the south, with a possible temporal lag.

Large-river deltas are dominant contributors to clastic sediment masses on continental shelves. Studying the along-shelf redistribution of sediments over the CSDDM will contribute to our understanding of land-coast-shelf system behavior, and will aid strategic assessments and flexible management of densely populated areas of great economic activity and rapid urbanization.

Acknowledgments

This study was supported by the Natural Science Foundation of China (Nos 41376068, 41776048 and 41625021). We are grateful to Yang Yang (SIOSOA), Yingfei Wang, Haijuan Cao, and Rui Yu for their assistance with fieldwork and laboratory analysis. Hui Sheng helped to redraw the maps and Chengfeng Xue collected additional data of sediment porosity and mean grain-size in the East China Sea. Two anonymous reviewers are particularly appreciated for their constructive and helpful suggestions and comments which are fairly helpful in revising the manuscript.

References

Alexander, C., DeMaster, D., Nittrouer, C., 1991. Sediment accumulation in a modern epicontinental-shelf setting: the Yellow Sea. Mar. Geol. 98 (1), 51–72.
Appleby, P.G., Oldfield, F., 1983. The assessment of ^{210}Pb data from sites with varying sediment accumulation rates. Hydrobiologia 103, 29–35.
Bianchi, T.S., Allison, M.A., 2009. Large-river delta-front estuaries as natural "recorders" of global environmental change. PNAS 106 (20), 8085–8092.
Chen, J. (Ed.), 2010. Comprehensive Survey Report on Coastal Zone Environment in Fujian Province. The Third Institute of Oceanography, State Oceanic Administration, China.
Chen, J.Y., Yun, C.X., Xu, H.G., Dong, Y.F., 1979. The developmental model of the Changjiang River Estuary during last 2000 years. China J. Oceanogr. 1 (1), 103–111 (in Chinese with English abstract).
Chen, Y.W., Zhao, Y.Y., Liu, J.Y., Qiu, J.G., 1982. Distribution characteristics of 226Ra in sediments of the East China Sea and determination of sedimentation rate in near-shore region. Oceanologia et Limnologia Sinica 13 (4), 380–387 (in Chinese with English abstract).
Chen, Z.Y., Saito, Y., Kanai, Y., Wei, T.Y., Li, L.Q., Yao, H.S., Wang, Z.H., 2004. Low concentration of heavy metals in the Yangtze estuarine sediments, China: a diluting setting. Estuar. Coast. Shelf Sci. 60 (1), 91–100.
Cheng, F.J., Yu, Z.M., Song, X.X., 2013. Variations of sediment grain size of the coastal mud area of the East China Sea and the influence factors during recent hundred years. Mar. Sci. 37 (10), 58–64 (in Chinese with English abstract).
Dai, Z.H. (Ed.), 1988. Technical Report on the Comprehensive Survey of Coastal Zone and Coastal Resources in Zhejiang Province. Ocean Press, Beijing.
Dai, S.B., Yang, S.L., Gao, A., Liu, Z., Li, P., Li, M., 2007. Trend of sediment flux of main rivers in China in the past 50 years. J. Sediment. Res. 2, 49–58.
DeMaster, D.J., Mckee, B.A., Nittrouer, C.A., Qian, J.C., Cheng, G.D., 1985. Rates of sediment accumulation and particle reworking based on radiochemical measurements from continental shelf deposits in the East China Sea. Cont. Shelf Res. 4 (1–2), 143–158.
Dong, A.G., Zhai, S.K., Zabel, M., Yu, Z.H., Chu, Z.X., 2009. Geochemistry characters of the core sediments in the Yangtze estuary and the response to human activities. Mar. Geol. Quat. Geol. 29 (4), 107–114 (in Chinese with English abstract).
Driscoll, N., Nittrouer, C., 2000. Source to sink studies. Margins Newsl. 5, 1–3.
Duan, L.Y., Wang, Z.H., Li, M.T., Pan, J.M., Chen, Z.Y., Saito, Y., Kanai, Y., 2005. ^{210}Pb distribution of the Changjiang estuarine sediment and the implications to sedimentary environment. Acta Sedimentol. Sin. 23 (3), 514–522 (in Chinese with English abstract).
Feng, X.W., Jin, X.L., Zhang, W.Y., Yu, X.G., Li, H.L., 2009. Variation of elements in sediments from the hypoxia zone of the Yangtze Estuary and its response to sedimentary environment over the last 100 years. Mar. Geol. Quat. Geol. 29 (2), 25–32 (in Chinese with English abstract).
Flemming, B.W., Delafontaine, M.T., 2000. Mass physical properties of muddy intertidal sediments: some applications, misapplications and non-applications. Cont. Shelf Res. 20, 1179–1197.
Gao, S., 2007. Modeling the growth limit of the Changjiang Delta. Geomorphology 85, 225–236.
Gao, S., 2010. Changjiang delta sedimentation in response to catchment discharge changes: progress and problems. Adv. Earth Science 25 (3), 233–241 (in Chinese with English abstract).
Gao, S., Collins, M.B., 2014. Holocene sedimentary systems on continental shelves. Mar. Geol. 352, 268–294.
Gao, S., Wang, Y.P., Gao, J.H., 2011. Sediment retention at the Changjiang sub-aqueous delta over a 57 year period, in response to catchment changes. Estuar. Coast. Shelf Sci. 95, 29–38.
Gao, J.H., Xu, X.N., Jia, J.J., Kettner, A.J., Xing, F., Wang, Y.P., Yang, Y., Zou, X.Q., Gao, S., Qi, S.H., Liao, F.Q., 2015a. A numerical investigation of freshwater and sediment discharge variations of Poyang Lake catchment, China over the last 1000 years. The Holocene 25 (9), 1470–1482.
Gao, J.H., Jia, J.J., Wang, Y.P., Yang, Y., Li, J., Bai, F.L., Zou, X.Q., Gao, S., 2015b. Variations in quantity, composition and grain size of Changjiang sediment discharging into the sea in response to human activities. Hydrol. Earth Syst. Sci. 19, 645–655.
Gao, S., Wang, D.D., Yang, Y., Zhou, L., Zhao, Y.Y., Gao, W.H., Han, Z.C., Yu, Q., Li, G.C., 2016. Holocene sedimentary systems on a broad continental shelf with abundant river input: process-product relationships. In: Clift, P.D., Harff, J., Wu, J., Yan, Q. (Eds.), River-dominated Shelf Sediments of East Asian Seas. Geological Society, London, Special Publications, vol. 429. pp. 223–259.
Gao, J.H., Jia, J.J., Sheng, H., Yu, R., Li, G.C., Wang, Y.P., Yang, Y., Zhao, Y.F., Li, J., Bai, F.L., Xie, W.J., Wang, A.J., Zou, X.Q., Gao, S., 2017. Variations in the transport, distribution and budget of 210Pb in sediment over the estuarine and inner shelf areas of the East China Sea due to Changjiang catchment changes. J. Geophys. Res. Earth Surf. 122 (1), 235–247.
Goldberg, E.D., 1963. Geochronology with ^{210}Pb. In: Radioactive Dating, Proceedings of the Symposium on Radioactive Dating Held by the International Atomic Energy Agency in Co-operation With the Joint Commission on Applied Radioactivity, Athens, (121-131 pp.).
Gu, G.C., Hu, F.X., Zhang, Z.T., 1997. The sediment source and development mechanics of the muddy coast in the East Zhejiang. Donghai Haiyang 15 (4), 1–12 (in Chinese with English abstract).
Hamilton, E.L., Bachman, R.T., 1982. Sound velocity and related properties of marine sediments. J. Acoust. Soc. Am. 72 (6), 1891–1904.
Huh, C.A., Chen, H.Y., 1999. History of lead pollution recorded in East China Sea sediments. Mar. Pollut. Bull. 38 (7), 545–549.
Huh, C.A., Chen, W., Hsu, F.H., Su, C.C., Chiu, J.K., Lin, S., Liu, C.H., Huang, B.J., 2011. Modern (< 100 years) sedimentation in the Taiwan Strait: rates and source-to-sink pathways elucidated from radionuclides and particle size distribution. Cont. Shelf Res. 31 (1), 47–63.
Jin, X.L., 1992. Submarine Geology of East China Sea. China Ocean Press, Beijing (524 pp.).
Jia, J.J., Gao, S., Xue, Y.C., 2003. Sediment dynamic behaviour of small tidal inlets: an example from Yuehu Inlet, Shandong Peninsula, China. Estuar. Coast. Shelf Sci. 57 (5–6), 783–801.
Jin, H.Y., Chen, J.F., Weng, H.X., Li, H.L., Zhang, W.Y., Xu, J., Bai, Y.C., Wang, K., 2009. Variations of paleoproductivity in the past decades and the environmental implications in the Changjiang Estuary in China. Acta Oceanol. Sin. 31 (2), 113–119 (in Chinese with English abstract).
Kao, S.J., Milliman, J.D., 2008. Water and sediment discharge from small mountainous rivers, Taiwan: the roles of lithology, episodic events, and human activities. J. Geol. 116 (5), 431–448.
Koide, M., Soutar, A., Goldberg, E.D., 1972. Marine geochronology with ^{210}Pb. Earth Planet. Sci. Lett. 14 (3), 442–446.
Lin, C.K., 1988. Quantity and transport of sediment at the Yangtze River Estuary. Sci. China, Ser. A 31 (12), 1495–1507.
Lin, J.L. (Ed.), 1990. Technical Report on the Comprehensive Survey of Coastal Zone and Coastal Resources in Fujian Province. Ocean Press, Beijing (in Chinese).
Lin, X.Y., Chu, Y.A., 1984. Preliminary analysis of the runoff emptying into the sea. Donghai Mar. Sci. 2 (4), 1–10 (in Chinese with English abstract).
Lin, C.K., Pan, S.M., 2005. When did the water of the Yangtze River become muddy in ancient times? Chin. J. Nat. 27 (1), 37–41 (in Chinese).
Li, Y.F., 1991. The development of the abandoned Yellow River delta. Geogr. Res. 10 (4), 29–39 (in Chinese with English abstract).
Li, B.H., Li, C.X., Shen, H.T., 2003. A preliminary study on sediment flux in the Changjiang Delta during the postglacial period. Sci. China Ser. D Earth Sci. 46 (7), 743–752.
Li, P., Yang, S.L., Dai, S.B., Zhang, W.X., 2007. Accretion/erosion of the subaqueous delta at the Yangtze Estuary in recent 10 years. Acta Geograph. Sin. 62 (7), 707–716 (in Chinese with English abstract).
Li, C.S., Shi, X.F., Gao, S.J., Liu, Y.G., Fang, X.S., Lü, H.H., Zou, J.J., Liu, S.F., Qiao, S.Q., 2012. Clay mineral composition and their sources for the fluvial sediments of Taiwanese rivers. Chin. Sci. Bull. 57 (6), 673–681.
Li, B., Yan, X.X., He, Z.F., et al., 2015. Impacts of the Three Gorges Dam on the bathymetric evolution of the Yangtze River Estuary. Chin. Sci. Bull. 60 (18), 1735–1744 (in Chinese with English abstract).
Liu, M., 2009a. High-resolution Sedimentary Records in the Subaqueous Yangtze River

Delta and Their Responses to Climate, Environment Changes. Ocean University of China, Qingdao (Master Dissertation, in Chinese with English abstract).
Liu, Y., 2009b. The Distribution and Environmental Significance of Environmental Labile Metal Element in the Mud Area of East China Sea. Ocean University of China, Qingdao (Master Dissertation, in Chinese with English abstract).
Liu, J.P., Li, A.C., Xu, K.H., Velozzi, D., Yang, Z.S., Milliman, J.D., DeMaster, D., 2006. Sedimentary features of the Yangtze River- derived along-shelf clinoform deposit in the East China Sea. Cont. Shelf Res. 26 (17–18), 2141–2156.
Liu, C., Wang, Z.Y., Sui, J.Y., 2007a. Analysis on variation of seagoing water and sediment discharge in main rivers of China. J. Hydraul. Eng. (SHUILI XUEBAO) 38 (12), 1444–1452 (in Chinese, with English abstract).
Liu, J.P., Xu, K.H., Li, A.C., Milliman, J.D., Velozzi, D., Xiao, S.B., Yang, Z.S., 2007b. Flux and fate of Yangtze River sediment delivered to the East China Sea. Geomorphology 85 (3–4), 208–224.
Liu, J.P., Liu, C.S., Xu, K.H., Milliman, J.D., Chiu, J.K., Kao, S.J., Lin, S.W., 2008. Flux and fate of small mountainous rivers derived sediments into the Taiwan Strait. Mar. Geol. 256 (1–4), 65–76.
Liu, J., Saito, Y., Kong, X.H., Wang, H., Xiang, L.H., Wen, C., Rakashima, R., 2010. Sedimentary record of environmental evolution off the Yangtze River estuary, East China Sea, during the last ~13000 years, with special reference to the influence of the Yellow River on the Yangtze River delta during the last 600 years. Quat. Sci. Rev. 29, 2424–2438.
Liu, J.T., Hsu, R.T., Yang, R.J., Wang, Y.P., Wu, H., Du, X.Q., Li, A.C., Chien, S.C., Lee, J., Yang, S.Y., Zhu, J.R., Su, C.C., Chang, Y., Huh, C.A., 2018. A comprehensive sediment dynamics study of a major mud belt system on the inner shelf along an energetic coast. Sci. Rep. 8, 4229. (2018). https://doi.org/10.1038/s41598-018-22696-w.
Milliman, J.D., Farnsworth, K.L., 2011. River Discharged to the Coastal Ocean: A Global Synthesis. Cambridge University Press, New York (384 pp.).
Milliman, J.D., Syvitski, J.P.M., 1992. Geomorphic/tectonic control of sediment discharge to the ocean: the importance of small mountainous rivers. J. Geol. 100, 525–544.
Milliman, J.D., Yang, Z.S., 2014. Chinese-U.S. sediment source-to-sink research in the east China and Yellow Seas: a brief history. Cont. Shelf Res. 90, 2–4.
Milliman, J.D., Shen, H.T., Yang, Z.S., Mead, R.H., 1985. Transport and deposition of river sediment in the Changjiang estuary and adjacent continental shelf. Cont. Shelf Res. 4 (1–2), 37–45.
Ministry of Water Resources of the People's Republic of China (MWR) Bulletin of River Sediment in China: 2000–2016. Press of Ministry of Water Resources of the People's Republic of China. Website: http://www.mwr.gov.cn/sj/tjgb/zghlnsgb/.
National Development and Reform Commission (NDRC), 2016. Development planning of city group in the Changjiang Delta. Website: http://www.ndrc.gov.cn/zcfb/zcfbghwb/201606/W020160715545638297734.pdf (in Chinese).
Nicholls, R.J., Cazenave, A., 2010. Sea-level rise and its impact on coastal zones. Science 328 (5985), 1517–1520.
Nittrouer, C.A., Sternberg, R.W., Carpenter, R., Bennett, J.T., 1979. The use of ^{210}Pb geochronology as a sedimentological tool: application to the Washington continental shelf. Mar. Geol. 31, 296–316.
Oguri, K., Matsumoto, E., Yamada, M., Saito, Y., Iseki, K., 2003. Sediment accumulation rates and budgets of depositing particles of the East China Sea. Deep-Sea Res. II Top. Stud. Oceanogr. 50 (2), 513–528.
Qin, Y.S., 1963. Preliminary study on the topography and sediment types over China marginal seas. Oceanologia et Limnologia Sinica 5 (1), 71–86 (in Chiness).
Qin, Y.S. (Ed.), 1996. Geology of The East China Sea. Science Press, Beijing.
Qin, Y.S., Zhao, Y.Y., Chen, L.R., Zhao, S.L. (Eds.), 1996. Geology of the East China Sea. Science Press, Beijing (in Chinese).
Qiao, F.L. (Ed.), 2012. Physical Oceanography of China Marginal Seas. Ocean Press, Beijing (in Chinese).
Qiao, S.Q., Shi, X.F., Wang, G.Q., Zhou, L., Hu, B.Q., Hu, L.M., Yang, G., Liu, Y.G., Yao, Z.Q., Liu, S.F., 2017. Sediment accumulation and budget in the Bohai Sea, Yellow Sea and East China Sea. Mar. Geol. 390, 270–281.
Ruan, M.N., Li, Y., Chen, Y.N., Chen, J.W., 2012. Summer pathways for suspended particles across the Taiwan Strait: evidence from the end-member analysis of in-situ particle size. Chin. Sci. Bull. (Chin Ver) 57 (36), 3522–3532 (in Chinese with English abstract).
Shi, X.F. (Ed.), 2012. Marine Sedimentation of China Marginal Seas. Ocean Press, Beijing (in Chinese).
Song, L., Xia, X.M., Liu, Y.F., Cai, T.L., 2012. Variations in water and sediment fluxes from Oujiang River to Estuary. J. Sediment. Res. 1, 46–52 (in Chinese, with English abstract).
Su, C.C., Huh, C.A., 2002. ^{210}Pb, ^{137}Cs and $^{239, 240}$Pu in East China Sea sediments: sources, pathways and budgets of sediments and radionuclides. Mar. Geol. 183, 163–178.
Syvitski, J.P.M., Morehead, M.D., 1999. Estimating river-sediment discharge to the ocean: application to the Eel margin, northern California. Mar. Geol. 154, 13–28.
Syvitski, J.P.M., Saito, Y., 2007. Morphodynamics of deltas under the influence of humans. Glob. Planet. Chang. 57, 261–282.
Syvitski, J.P.M., Kettner, A.J., Overeem, I., Hutton, E.W.H., Hannon, M.T., Brakenridge, G.R., Day, J., Vörösmarty, C., Saito, Y., Giasan, L., Nicholls, R.J., 2009. Sinking deltas due to human activities. Nat. Geosci. 2 (10), 681–686.
Tanner, P.A., Pan, S.M., Mao, S.Y., Yu, K.N., 2000. γ-Ray spectrometric and α-counting method comparison for the determination of Pb-210 in estuarine sediments. Appl. Spectrosc. 54 (10), 1443–1446.
Tao, C.H., 2011. Pilot study and application demonstration of non-contact survey on the qualitative analysis of surficial sediment using acoustic instrument. In: The Second Institute of Oceanography, State Oceanic Administration: Research Report, (in Chinese).
Wang, H.J., Yang, Z.S., Wang, Y., Saito, Y., Liu, P., 2008. Reconstruction of sediment flux from the Changjiang (Yangtze River) to the sea since the 1860s. J. Hydrol. 349, 318–332.
Wang, J., Bai, S.B., Liu, P., Li, Y.Y., Gao, Z.R., Qu, G.X., Cao, G.J., 2009. Channel sedimentation and erosion of the Jiangsu reach of the Yangtze River during the last 44 years. Earth Surf. Process. Landf. 34, 1587–1593.
Wang, X., Shi, X.F., Liu, S.F., Wang, G.Q., Qiao, S.Q., Zhu, A.M., Gao, J.J., 2012. High resolution sedimentary record within a hundred years on the mud area near the Changjiang estuary and discussion of its impacting factors. Acta Sedimentol. Sin. 30 (1), 148–157 (In Chinese with English abstract).
Wang, X., Shi, X.F., Liu, S.F., Wang, G.Q., Qiao, S.Q., Liu, T., 2013. Sedimentation rates and its indication to distribution of Yangtze sediment supply around the Yangtze (Changjiang) River estuary and its adjacent area, China. Earth Sci. J. China Univ. Geosci. 38 (4), 763–775 (In Chinese with English abstract).
Wang, Y.P., Gao, S., Jia, J.J., Liu, Y.L., Gao, J.H., 2014. Remarked morphological change in a large tidal inlet with low sediment-supply. Cont. Shelf Res. 90, 79–95.
Wang, J.L., Du, J.Z., Baskaran, M., Zhang, J., 2016. Mobile mud dynamics in the East China Sea elucidated using Pb-210, Cs-137, Be-7, and Th-234 as tracers. J. Geophys. Res. Oceans 121 (1), 224–239.
Wu, H., Gu, J., Zhu, P., 2018. Winter counter-wind transport in the inner southwestern Yellow Sea. J. Geophys. Res. Oceans 123, 411–436.
Xing, F., Wang, Y.P., Wang, H.V., 2012. Tidal hydrodynamics and fine-grained sediment transport on the radial sand ridge system in the southern Yellow Sea. Mar. Geol. 291, 192–210.
Xing, F., Kettner, A.J., Ashton, A., Giosan, L., Ibáñez, C., Kaplan, J.O., 2014. Fluvial response to climate variations and anthropogenic perturbations for the Ebro River, Spain in the last 4000 years. Sci. Total Environ. 473-474, 20–31.
Xia, X.M. (Ed.), 2011. Comprehensive Survey Report on Coastal Zone Environment in Zhejiang Province. The Second Institute of Oceanography, State Oceanic Administration, China.
Xia, X.M., Xie, Q.C., Li, Y., Li, B.G., Feng, Y.J., 1999. 137Cs and 210Pb profiles of the seabed cores along the East China Sea coast and their implications to sedimentary environment. Donghai Mar. Sci. 17 (4), 20–27 (in Chinese with English abstract).
Xia, X.M., Yang, H., Li, Y., Li, B.G., Pang, S.M., 2004. Modern sedimentation rates in the contiguous sea area of Changjiang Estuary and Hangzhou Bay. Acta Sedimentol. Sin. 22 (1), 130–134 (in Chinese).
Xie, W.J., 2013. Characteristics and Sediment Dynamical Factors of 210Pb Vertical Profiles of Surficial Sediments Over the Changjiang Subaqueous Delta. Nanjing University, Nanjing (Ph.D. Dissertation).
Xie, Q.C., Li, B.G., Xia, X.M., Li, Y., Van Weering, T.C.E., Berger, G.W., 1994. Spatial and temporal varlations of tidal flat in the Oujiang estuary in China. Acta Geograph. Sin. 49 (6), 509–516 (in Chinese with English abstract).
Xie, Q.C., Ma, L.M., Li, B.G., Yang, H., 2001. Rapid storm sedimentation of Maotou deep trough in the Sanmen Bay of Zhejiang. Acta Oceanol. Sin. 23 (5), 78–86 (in Chinese with English abstract).
Xu, S.Y., 2000. The Consulting Report on the Environment and Resource Structure and Regulation of Coastal Zone in Shanghai. East China Normal University (in Chinese).
Xu, C.X., Zhou, B.S., 2004. Current situation and prospect of beach reclamation in Zhejiang province. Donghai Mar. Sci. 22 (2), 53–58.
Xu, K.H., Milliman, J.D., Li, A.C., Liu, P., Kao, S.J., Wan, S.M., 2009. Yangtze- and Taiwan-derived sediments on the inner shelf of East China Sea. Cont. Shelf Res. 29, 2240–2256.
Xu, K.H., Li, A.C., Liu, P., Milliman, J.D., Yang, Z.S., Liu, C.S., Kao, S.J., Wan, S.M., Xu, F.J., 2012. Provenance, structure, and formation of the mud wedge along inner continental shelf of the East China Sea: a synthesis of the Yangtze dispersal system. Mar. Geol. 291-294, 176–191.
Yang, Z.S., Chen, X.H., 2007. Centurial high resolution record of sediment grain-size variations in the mud area off the Changjiang (Yangtze River) estuary and its influencial factors. Quat. Sci. 27 (5), 690–699 (in Chinese with English abstract).
Yang, S.L., Zhu, J., Zhao, Q.Y., 2003. A preliminary study on the influence of Changjiang River sediment supply on subaqueous delta. Acta Oceanol. Sin. 25 (5), 83–91 (in Chinese with English abstract).
Yang, S.L., Milliman, J.D., Li, P., Xu, K., 2011. 50,000 dams later: erosion of the Yangtze River and its delta. Glob. Planet. Chang. 75 (1–2), 14–20.
Youn, J.S., Kim, T.J., 2011. Geochemical composition and provenance of muddy shelf deposits in the East China Sea. Quat. Int. 230 (1–2), 3–12.
Yu, Q., Wang, Y.W., Gao, S., 2014. Tide and continental shelf circulation induced suspended sediment transport on the Jiangsu Coast: winter observations out of Xinyanggang. J. Nanjing Univ. (Nat. Sci.) 50 (5), 626–635 (in Chinese with English abstract).
Zhan, Q., Wang, Z.H., Chen, Y., Zhao, B.C., 2016. Grain size of recent sediments in Yangtze River subaqueous delta and its response to sediments supply decline. Geol. Bull. China 35 (10), 1715–1723 (in Chinese with English abstract).
Zhang, R.S., 1984. Land forming history of the Huanghe (Yellow) River delta and coastal plain of north Jiangsu. Acta Geograph. Sin. 39 (2), 173–184 (in Chinese with English abstract).
Zhang, J., 2008. Comparison Research on the Sedimentation Rate in the Changjiang Estuary and Its Adjacent Area. East China Normal University, Shanghai (Master Dissertation, in Chinese with English abstract).
Zhang, Z.Z., Li, S.L., Dong, Y.X., Wang, Q.H., Xiao, F., Lu, J., 2005. Deposition rate and geochemical characters of sediments in Zhejiang offshore. Mar. Geol. Quat. Geol. 25 (3), 15–24 (in Chinese with English abstract).
Zhang, R., Pan, S.M., Wang, Y.P., Gao, J.H., 2009. Sedimentation rates and characteristics of radionuclide ^{210}Pb at the subaqueous delta in Changjiang Estuary. Acta Sedimentol. Sin. 27 (4), 704–771 (in Chinese with English abstract).
Zhang, Z., Liu, J., Chen, B., Xu, G., Qiu, J.D., Wang, S., 2016. Depositional records of heavy metals for the last 140 years in the Zhejiang coastal muddy area of the Yangtze

River basin and their responses to human activities. Mar. Geol. Quat. Geol. 36 (3), 23–33 (in Chinese with English abstract).
Zhejiang Administration of Surveying, Mapping and Geoinformation (ZJSMG), 2010. Bulletin on the geographical data of length and drainage area of main rivers and of area of main lakes in Zhejiang Province. http://www.zjch.gov.cn/xxgk/jcms_files/jcms1/web1/site/art/2010/10/13/art_71_1712.html (online).
Zhou, X.J., Gao, S., Jia, J.J., 2003. Preliminary evaluation of the stability of Changjiang clay minerals as fingerprints for material source tracing. Oceanologia et Limnologia Sinica 34 (6), 683–692 (in Chinese with English abstract).